Published in final edited form as:
Inorg Chem. 2010 June 21; 49(12): 5766–5774. doi:10.1021/ic100730j.

Synthesis and Characterization of Free-Base, Copper and Nickel Isocorroles

Giuseppe Pomarico[1], **Xiao Xiao**[3], **Sara Nardis**[1], **Roberto Paolesse**[1,*], **Frank R. Fronczek**[2], **Kevin M. Smith**[2,*], **Yuanyuan Fang**[3], **Zhongping Ou**[3], and **Karl M. Kadish**[3,*]

[1]Dipartimento di Scienze e Tecnologie Chimiche, Università di Roma Tor Vergata, via della Ricerca Scientifica, 1, 00133 Rome, Italy

[2]Department of Chemistry, Louisiana State University, Baton Rouge, Louisiana 70803 USA

[3]Department of Chemistry, University of Houston, Houston, Texas 77204-5003 USA

Abstract

A series of free-base and metalated isocorroles represented as (TT-*n*-iso-Cor)H_2 and (TT-*n*-iso-Cor)M^{II}, where *n* = 5 or 10 and M = Ni or Cu, were synthesized and characterized by electrochemistry and spectroelectrochemistry in CH_2Cl_2 containing 0.1 M TBAP. A metalation of the free-base macrocycles with Co^{II}, Mn^{III} or Zn^{II} was also attempted but was unsuccessful. Five isocorroles were isolated and shown to undergo two stepwise oxidations to give π-cation radicals and dications in CH_2Cl_2, with the most stable products being obtained in the case of the 10-substituted derivatives. The same isocorroles could also be reduced by one or two electrons but the initial one-electron addition products are unstable and undergo a rapid chemical reaction giving a reduced corrole or corrole-like product, which could be reoxidized to the corresponding (TTCor)M at a controlled positive potential. This series of reactions effectively gives an isocorrole to corrole conversion upon reduction and reoxidation and was monitored by both electrochemistry and thin-layer spectroelectrochemistry.

Introduction

Porphyrins represent the prototypical example of a pyrrolic macrocycle due to their essential biological functions. Related families of the so called “porphyrinoids” are also known and available from both natural and synthetic sources. These macrocycles differ from the well-characterized porphyrins by one or more structural elements, examples being in the number of pyrrole rings,[1] in having one or more of the pyrrole rings replaced by a furan or thiopene group[2] or by the macrocycle having a different number or position of the meso-bridges as compared to the porphyrins.[3,4] There are also several examples of porphyrinoid macrocycles where the aromatic system is interrupted, one example is given by isoporphyrins[5] where the conjugation pathway is interrupted by the presence of a saturated meso-carbon as shown in Chart 1.

Currently, the most frequently studied porphyrin analogues are the corroles which have acquired a special interest because of their particular behavior which leads to possible applications in the area of catalysis or sensors.[6–9] Recent advances in the synthetic

roberto.paolesse@uniroma2.it; kkadish@uh.edu; kmsmith@lsu.edu.

SUPPORTING INFORMATION. Mass spectra, Cyclic voltammograms, the UV-visible spectral changes obtained during controlled potential reductions or oxidations in CH_2Cl_2, 0.1 M TBAP and CIF of (TT-10-isoCor)Cu. This material is available free of charge via the internet at http://pubs.acs.org.

chemistry of corroles have also allowed for the preparation of other related analogues, one of which is the isocorrole which may exist in two isomeric forms as shown in Figure 2.

The first synthesis of a free-base isocorrole was reported in 2006 by Setsune10 but the idea was earlier discussed in a paper by Vogel and collaborators as it related to a Ni isocorrole derivative.11 More recently, Setsune reported the synthesis and characterization of several metal isocorrole complexes.[12] It should also be noted that the term "porphyrinoid [0.2.0.1]" has been used to indicate an isocorrole.[13,14] The isocorrole has also been called a "pseudocorrole".15 However, for the sake of consistency with the isoporphyrins, the term isocorrole will be used to describe the compounds reported in this present paper.

Our own laboratory has followed a synthetic route different from that described in the literature for isocorrole preparation and was based on the readily available meso triaryl-corrole as a precursor.[16] This analogue was prepared via a one-step reaction involving oxidation of the starting corrole with DDQ in the presence of a nucleophile, usually methanol. The route provides a simple approach to obtain a wide range of different isocorroles and is important when considering the remarkable development in new synthetic routes for obtaining corroles bearing aryl substituents.[17–20] It is also possible with this synthetic method to prepare the 5-isomers which have been only recently been reported.[21]

The presence of a methoxy or a hydroxy substituent instead of an alkyl group at the meso-positions of an isocorrole makes possible an isocorrole-corrole conversion upon metal coordination. We observed this effect after bromination of free-base triphenylcorrole where an oxidation of the macrocycle led to the corresponding isocorrole species, which then could be converted back to the parent corrole during coordination with Co(III).[19] This feature prompted us to further investigate the behavior of the non-aromatic isocorrole as a chelate, exploring also its stability when reacted with different metal ions. This is described in the present paper where we report the synthesis, electrochemistry and spectroelectrochemistry of five free-base or metalated isocorroles represented as (TT-*n*-iso-Cor)H_2 and (TT-*n*-iso-Cor)M^{II} where n = 5 or 10 and M = Ni or Cu.

Experimental

Chemicals

Reagents and solvents (Sigma-Aldrich, Fluka and Carlo Erba Reagenti) were of synthetic grade and used without further purification. Silica gel 60 (70–230 mesh) was used for chromatography. Dichloromethane (CH_2Cl_2, 99.8%) was purchased from EMD Chemicals Inc. and used as received. Tetra-*n*-butylammonium perchlorate (TBAP) was purchased from Sigma Chemical or Fluka Chemika Co., recrystallized from ethyl alcohol, and dried under vacuum at 40 °C for at least one week prior to use.

Instrumentation

^{1}H NMR spectra were recorded on a Bruker AV300 (300 MHz) spectrometer. Chemical shifts are given in ppm relative to tetramethylsilane (TMS). UV-vis spectra were measured on a Cary 50 spectrophotometer or with an HP Model 8453 diode array spectrophotometer (Hewlett Packard Company). High resolution mass spectra were recorded on a Voyager DE STR Biospectrometry workstation in the positive mode, using α-cyano-4-hydroxycinnamic acid as a matrix (MALDI).

Cyclic voltammetry was carried out at 298 K by using an EG&G Princeton Applied Research (PAR) 173 potentiostat/galvanostat. A homemade three-electrode cell was used for cyclic voltammetric measurements and consisted of a glassy carbon working electrode, a platinum counter electrode and a homemade saturated calomel reference electrode (SCE).

The SCE was separated from the bulk of the solution by a fritted glass bridge of low porosity which contained the solvent/supporting electrolyte mixture.

Thin-layer UV-visible spectroelectrochemical experiments were performed with a home-built thin-layer cell which has a light transparent platinum net working electrode. Potentials were applied and monitored with an EG&G PAR Model 173 potentiostat. Time-resolved UV-visible spectra were recorded with a Hewlett-Packard Model 8453 diode array spectrophotometer. High purity N_2 from Trigas was used to deoxygenate the solution and kept over the solution during each electrochemical and spectroelectrochemical experiment.

General procedure for preparation of 5- and 10-methoxy-5,10,15-tritolyl-isocorroles, (TT-5-isoCor)H_2 and (TT-10-isoCor)H_2

In a 100 mL round-bottomed flask, equipped with a stirring bar, tritolylcorrole (50 mg, 0.088 mmol) was dissolved in 30 mL of dichloromethane/methanol mixture (2:1); DDQ (20 mg, 0.088 mmol) was added and the mixture was stirred for about 5 minutes, monitoring the progress of the reaction by UV-vis spectroscopy and TLC. After disappearance of the starting material, the solvent was evaporated under vacuum and the crude product dissolved with CH_2Cl_2 and passed on a short silica gel plug eluted with CH_2Cl_2. A green fraction containing the two isomers was collected and crystallized from CH_2Cl_2/CH_3OH. If separation of mixture was required, isomers were purified by preparative layer chromatography (silica gel, CH_2Cl_2-Hexane 2:1 as eluent). The first light green fraction corresponds to isomers 10, the second dark green to the isomer 5 and either crystallized from CH_2Cl_2/CH_3OH. Overall yield: 75% (40 mg); isomer ratio: H_2TT-10-isoCor: 34% (13.5 mg); (TT-5-isoCor)H_2: 66% (26.5 mg). Spectroscopic data have been previously reported in literature.[16]

General procedure for preparation of isocorrole Copper complexes

Mixture of isocorrole was dissolved in CH_2Cl_2, and a few mLs of a saturated solution of $Cu(OAc)_2$ in CH_3OH were added. Mixture was stirred to reflux for 45 minutes and the course of the reaction monitored by UV-vis spectroscopy and TLC (silica gel, CH_2Cl_2-Hexane 2:1) After disappearance of starting material, solvent was removed under reduced pressure, residue purified by PLC (silica gel, CH_2Cl_2-Hexane 2:1). Two fractions were collected, the first corresponding to isomer 10, and the second to isomer 5.

(10-Methoxy-5,10,15-tritolyl-isocorrolato)Cu, (TT-10-isoCor)Cu)

The orange fraction was crystallized from CH_2Cl_2/CH_3OH (yield 27%). Found: C, 74.3; H, 5.1; N, 8.4; $C_{41}H_{32}CuN_4O$ required C, 74.6; H, 4.9; N, 8.5. UV-vis: $\lambda_{max}(CH_2Cl_2)$, nm 371 (log ε, 4.54), 418 (4.50), 472 (4.57), 543 (3.75), 749 (3.58); 795 (3.70); 828 (3.97); HRMS (MALDI): m/z 658.6965, (M^+), 627.6692, (M-OCH_3). Crystallographic data: $C_{41}H_{32}N_4O.CHCl_3$, triclinic space group P-1, a=7.6453(8), b=11.2802(10), c=21.863(2) Å, α=79.320(6), β=85.260(6), γ=70.830(9)°, V=1749.6(3) $Å^3$, Z=2, ρ_{calcd}=1.480 g cm^{-3}, μ(CuKα)=3.313 mm^{-1}, R_{int}=0.039, R=0.050 (4817 data with $Fo^2>2\sigma(Fo^2)$), Rw=0.134 (all 6194 unique data) and 433 refined parameters. A total of 15,861 data was collected at T=90.0(5) K to θ=68.7° with CuKα radiation (λ=1.54178 Å) on a Bruker Kappa Apex-II diffractometer, using an orange lath crystal of dimensions 0.22×0.11×0.02 mm. Refinement was by full-matrix least squares using SHELXL, with H atoms in idealized positions. The chloroform is disordered, and its contribution to the structure factors was removed using SQUEEZE.[22] The phenyl group adjacent to methoxy is disordered into two orientations with nearly equal refined occupancies, 0.529(6)/0.471(6). CCDC-762432 contains the supplementary crystallographic data for this paper. These data can be obtained online free of charge (or from the Cambridge Crystallographic Data Centre, 12, Union Road, Cambridge CB2 1EZ, UK; fax: (+44) 1223-336-033; or deposit@ccdc.cam.ac.uk).

(5-Methoxy-5,10,15-tritolyl-isocorrolato)Cu, (TT-5-isoCor)Cu

The brown fraction was crystallized from CH_2Cl_2/CH_3OH (yield 54%). Found: C, 74.4; H, 5.2; N, 8.3; $C_{41}H_{32}CuN_4O$ requires C, 74.6; H, 4.9; N, 8.5. UV-vis: $\lambda_{max}(CH_2Cl_2)$, nm 358 (log ε, 4.31), 415 (4.57), 462 (4.30), 541 (3.75), 569 (3.67); 610 (3.45); 820 (3.53); HRMS (MALDI): m/z 658.2563, (M^+), 627.4931, (M-OCH_3).

General procedure for preparation of isocorrole Nickel complexes

Mixture of isocorroles was dissolved in DMF, and a three-fold excess of $Ni(OAc)_2$ was added. Mixture was stirred to reflux for 3 h and the course of the reaction monitored by UV-vis spectroscopy and TLC (silica gel, CH_2Cl_2-Hexane 2:1). After the disappearance of starting material, mixture was left to cool and then precipitate with water and filtered on paper. Residue was dissolved with CH_2Cl_2, dried over Na_2SO_4, and purified with a silica gel plug eluted with CH_2Cl_2, then purified again by PLC (silica gel, CH_2Cl_2-Hexane 2:1) in order to separate the isomers. Two fractions were collected, the first brown corresponding to the 10 isomer and the second green to the 5 isomer.

[10-Methoxy-5,10,15-tritolyl-isocorrolato]Ni, (TT-10-isoCor)Ni

The brown fraction was crystallized from CH_2Cl_2/CH_3OH (yield 49%). Found: C, 74.9; H, 5.0; N, 8.3; $C_{41}H_{32}N_4NiO$ required C, 75.1; H, 4.9; N, 8.5. UV-vis: $\lambda_{max}(CH_2Cl_2)$, nm 361 (log ε, 4.30), 409 (4.51), 430 (4.54), 442 (4.59), 531 (3.86); 560 (3.82); 602 (3.70); 818 (3.45); 905 (4.10); ^1H NMR $\delta_{ppm}(CDCl_3, J$ [Hz]) 7.76 (2 H, d, J = 8.18, 10-phenyl); 7.32 (4 H, m, 5,15-pheyl); 7.19 (4 H, m, 5,15-phenyl); 7.11 (2 H, d, J = 8.03, 10-phenyl); 6.44 (2 H, d, J = 4.50, β-pyrrole); 6.28 (2 H, d, J = 4.35, β-pyrrole); 6.24 (2 H, d, J = 4.20, β-pyrrole); 6.15 (2 H, d, J = 4.44, β-pyrrole); 3.40 (3 H, s, 10-OCH_3); 2.42 (6 H, s, 5 and 15-phenyl-CH_3); 2.30 (3 H, s, 10-phenyl-CH_3). MS (MALDI): m/z 654.0038, (M^+), 624.0842, (M-OCH_3).

[5-Methoxy-5,10,15-tritolyl-isocorrolato]Ni, (TT-5-isoCor)Ni

The brown fraction was crystallized from CH_2Cl_2/ CH_3OH (yield 32%). Found: C, 75.0; H, 5.1; N, 8.3; $C_{41}H_{32}N_4NiO$ required C, 75.1; H, 4.9; N, 8.5. UV-vis: $\lambda_{max}(CH_2Cl_2)$, nm 402 (log ε, 4.53), 447 (4.66), 677 (3.69), 866 (3.75), 967 (3.90); ^1H NMR $\delta_{ppm}(CDCl_3, J$ [Hz]) 7.73 (2 H, d, J = 8.15, 10-phenyl); 7.22 (8 H, m, 5 and 15-phenyl); 7.07 (2 H, d, J = 8.2, 10-phenyl); 6.51 (1 H, d, J = 4.90, β-pyrrole); 6.41 (4 H, m, β-pyrrole); 6.26 (1 H, d, J = 4.54, β-pyrrole); 6.22 (1 H, d, J = 4.54, β-pyrrole); 5.85 (1 H, d, J = 3.94, β-pyrrole); 3.45 (3 H, s, 5-OCH_3); 2.42 (3 H, s, phenyl-CH_3); 2.40 (3 H, s, phenyl-CH_3); 2.30 (3 H, s, phenyl-CH_3). MS (MALDI): m/z 653.8926, (M^+), 623.7804, (M-OCH_3).

[5,10,15-tritolyl-corrolato]Ni, (TTCor)Ni

Tritolyl-corrole (30 mg, 0.053 mmol) was dissolved in DMF and $Ni(OAc)_2$ was added. Mixture was stirred under refluxing for 2 hours, monitoring the course by UV-vis spectroscopy and TLC (silica gel, CH_2Cl_2:Hexane 2:1). After disappearance of corrole free base, mixture was left to cool down then precipitated with water and filter; residue was dissolved with chloroform, dried over Na_2SO_4 and purified by a silica gel column eluted with CH_2Cl_2. First brown band, corresponding to NiTTC was crystallized by CH_2Cl_2/ CH_3OH, giving 21 mg (0.034 mmol) of brownish crystals (Yield: 65%). Found: C, 76.8; H, 5.1; N, 8.7; $C_{40}H_{29}N_4Ni$ required C, 77.0; H, 5.0; N, 8.8. UV-vis: $\lambda_{max}(CH_2Cl_2)$, nm 387 (log ε, 4.56), 445 (4.61), 547 (4.12), 705 (3.85), 867 (3.62).

Results and Discussion

Synthesis and characterization

The coordination behavior of (TT-10-isoCor)H_2 and (TT-5-isoCor)H_2 was examined by reaction with the following metal ions: Co^{II}, Mn^{III}, Cu^{II}, Ni^{II} and Zn^{II}. The choice of these metals was due to their different formal oxidation states when coordinated to a corrole species: cobalt and manganese usually have formal oxidation states higher than +2, while in the case of copper and nickel an equilibrium between the +2 and +3 oxidation states can occur. A +2 oxidation state is always observed in the case of zinc.[23] Our aim was to investigate the stability of isocorrole complex against its conversion to the corresponding corrole derivative; we would expect a metal to ligand electron transfer in the case of metals adopting formal oxidation states higher than +2, with a consequent rearomatization to the corrole upon reduction of the isocorrole species.

The first metalation attempt was with cobalt ion, which has already been demonstrated to induce the corrole formation when coordinated to a free-base isocorrole.[19,24] We reacted a mixture of (TT-10-isoCor)H_2 and (TT-5-isoCor)H_2 dissolved in CH_2Cl_2 with a saturated solution of $Co(OAc)_2$ and triphenylphosphine in methanol, obtaining a single reaction product. UV-vis spectroscopy strongly suggested that the cobalt ion induced a re-aromatization of the macrocycle, this hypothesis being supported by comparison with a sample of authentic (TTCor)Co(PPh_3).

This result confirmed what was previously observed for other metal ions (see above), but considering the peculiar affinity showed by Co ion with the corrole framework, we decided to study the generality of this reaction using in this coordination with Mn ion which assumes a formal oxidation state higher than +2 when coordinated to corroles.[23] This could then provide further support for the generality of the isocorrole to corrole conversion. The reaction was carried out in refluxing DMF under an inert atmosphere using $MnCl_2$ as metal carrier. The reaction afforded a brown product, which was compared with a pure sample of (TTCor)Mn, showing identical spectroscopic features.

The conversion of an isocorrole to a corrole upon coordination of a high oxidation state metal could be reasonably attributed to the pathway shown in Scheme 1 for the case of the manganese derivative. After metalation of the isocorrole, an oxidation of the central metal ion is proposed to occur and this would be accompanied by reduction at the isocorrole π ring system to give the corresponding corrole after rearomatization of the macrocycle and loss of OCH_3 which was not identified in the reaction mixture.

The second metal ion insertion examined in the present study was copper whose electronic state in the corrole is still a matter of debate, being either Cu(III) or Cu(II) depending upon the oxidation state of the corrole macrocycle.[25–30] The equilibrium shown in Eq. 1 has been proposed and is supported by the diamagnetic character of Cu triarylcorrolates at room temperature,28 although it has been suggested[30] that caution be used for characterization of such a species. Nonetheless a comparison of the currently investigated compounds with Cu(II) 10-oxacorrole, suggests that copper ion in the overall neutral corrole molecule can be best described as Cu(II).[30]

$$(Cor)Cu^{III} \leftrightarrows (Cor^{+\cdot})Cu^{II} \quad (1)$$

Metalation of the isocorrole with Cu(II) was carried out in refluxing CH_2Cl_2 solution using a mixture of isocorrole regioisomers, to which was added a few milliliters of saturated copper

acetate in methanol. Three products were observed by TLC after disappearance of the starting material. The first was characterized as (TTCor)Cu, suggesting a similar isocorrole to corrole conversion as when metalation attempts were made with cobalt or manganese and gave a (TTCor)Mn or (TTCor)Co product.

A second band in the mixture after reacting the isocorrole with copper acetate (TLC, silica gel eluted with CH_2Cl_2 : hexane 2 : 1) was orange in color, while a more intense third band was red-brown. After separation by chromatography, the orange fraction was subsequently identified as the 10-isomer and has three Soret-like bands existing in the blue-green portion of the visible region (380–500 nm). The 5-isomer has a single soret band at 415 nm, with a shoulder at a higher wavelength and a weak absorption shifted towards the blue portion of the spectrum (Fig. 1).

An unambiguous ^1H NMR characterization of the two isocorrole regioisomers was not possible due to the paramagnetic behavior of the copper complexes, as expected for a species having a Cu(II) ion coordinated within the isocorrole macrocycle.

We initially assumed that the first collected orange product was the 10-isomer and the second red-brown species the 5-isomer, an assignment based on the fact that the two complexes have the same R_f value as the corresponding free-base forms of these isomers. To confirm this hypothesis, we repeated copper insertion experiments using separately the 5- and 10- isomers. In both cases, together with a small quantity of (TTCor)Cu, we obtained products identical to those previously isolated, confirming that the first eluted band corresponds to (TT-10-isoCor)Cu and the second to (TT-5-isoCor)Cu. Mass spectra of both the 5- and 10- isocorrole isomers showed a molecular peak at 660 M/Z^+, corresponding to the copper isocorrole complex, with a parent peak at 627 M/Z^+, corresponding to the loss of the methoxy group (see Fig. S1). We were able to obtain a single crystal of (TT-10-isoCor)Cu suitable for X-ray characterization by slow diffusion of methanol into a dichloromethane solution.

The molecular structure is shown in Figure 2, which illustrates only one of the two disordered MePh orientations. The coordination geometry is square planar, with the Cu atom lying 0.0027(7) Å out of the best plane of the four N atoms, which exhibit a maximum deviation of 0.007(3) Å from coplanarity. The Cu-N distances in the five-membered chelate ring are 1.914(2) and 1.915(2) Å, while those in the six-membered chelate ring containing the sp3 C atom are 1.923(3) and 1.929(2) Å. These distances are all longer than typical Cu-N distances in Cu(III) corroles, which show a mean value of 1.892 Å for 44 individual distances from Cambridge Structural Database31 entries BERVOK, BINCUX, FATDOU, FATDUA, FATFAI, GEDQAI, KAGGIJ, QEVQAK, and RINCAS. The average Cu-N length difference is in accord with the approximate 0.03 Å larger ionic radius of square-planar Cu(II) vs. Cu(III). The distances observed in Cu(TT-10-isoCor) are, however, slightly shorter than those seen in Cu(II) porphyrins on account of the contracted ring of the isocorrole. For example, the Cu-N bond distance in Cu(tetraphenylporphyrin)32 is 1.995(2) Å, identical to the mean value of 1.996 Å seen in several Cu(II) tetraalkylporphyrins.33 Overall, the 23-atom isocorrole core in Cu(TT-10-isoCor) deviates slightly from planarity, with mean deviation 0.114 Å, the maximum being the sp3 C atom, which lies 0.264(5) Å from the best plane.

The formation of a metalated isocorrole depends on both the reaction time and the temperature. Insertion of copper does not require harsh conditions but when the reaction mixture was heated for more than two hours, the amount of (TTCor)Cu increased significantly. This feature was confirmed by carrying out the reaction in the higher boiling DMF solvent using $CuCl_2$ as a metal carrier. After two hours in refluxing DMF, (TTCor)Cu

was detected as the main reaction product while only trace amounts of copper isocorrole were found in the mixture.

We then attempted insertion of Ni and Zn ions, both of which would be in the +2 oxidation state, perhaps facilitating formation of a stable metalated isocorrole. Our initial choice was Zn(II) ion because of its facile insertion into porphyrins. The same synthetic approach as described above was used, namely refluxing the mixture of isocorrole regioisomers in CH_2Cl_2 and adding of few ml of saturated $Zn(OAc)_2$ in methanol.

The UV-vis spectral changes which immediately occur after Zn(II) addition indicate that metalation has taken place, but all attempts to isolate the Zn isocorrole failed and the product quickly decomposed during reaction work up. After that we turned out our attention to Ni(II) which we hoped would form stable and diamagnetic compounds, making easier the product characterization. The isocorrole regiosomers and $Ni(OAc)_2$ were dissolved in DMF and the mixture heated to reflux for three hours while monitoring the course of the reaction by UV-vis spectroscopy and TLC (silica gel, CH_2Cl_2:hexane 2:1 as eluent). The reaction gave a brownish product that was quickly purified by a silica gel plug and eluted with dichloromethane to separate the desired isocorroles from the side products. Two fractions were isolated by preparative TLC (silica gel, CH_2Cl_2-hexane 2:1) and these eluted in an order suggesting formation of the 10- and 5-isocorrole Ni complexes, respectively. Their UV-vis spectra are reported in Figure 3.

The two regioisomers were identified by ^{1}H NMR spectroscopy, an example of which is given in Figure 4. The ^{1}H NMR spectrum of Ni(TT-10-isoCor) shows a signal pattern characterized by a higher symmetry than that of Ni(TT-5-isoCor) and one can note multiple signals of the β-pyrrole and the presence of three different signals referred to methyl substituents on the meso-phenyl groups.

We also attempted Ni metalation using the already separated isocorrole isomers and obtained the same products as when the reaction was carried out using the isomeric mixture. No rearrangement of the isomers was observed upon metalation, thus allowing preparation of the isocorroles using directly the isomer mixture.

Electrochemistry

Redox properties of the isocorroles and the related metallocorroles were examined in CH_2Cl_2 containing 0.1 M TBAP and examples of cyclic voltammograms are shown in Figure 5a for the three (TT-isoCor)M derivatives where M = 2H, Ni(II) or Cu(II). Each isocorrole derivative undergoes two reversible one electron oxidations at the conjugated macrocycle and one or two isocorrole-centered reductions, the latter of which are followed by a rapid chemical reaction on the electrochemical timescale. Other redox processes are also seen in the cyclic voltammograms and these are associated with reactions of a “corrole side product” as determined by comparison with data in the literature for genuine corroles[23,34] and that of (TTCor)Ni or (TTCor)Cu whose cyclic voltammograms are shown in Figure 5b.

The formal M(III)/M(II) processes of (TTCor)M are located at +0.02 V(Ni) or −0.23 V(Cu) (Figure 5b) and electrode reactions at the same potentials are seen in the Ni and Cu isocorrole cyclic voltammograms of Figure 5a. Additional reductions of the corrole beyond the M^{III}/M^{II} processes are not observed up to potentials of almost −2.00 V vs SCE[34] (see Fig. 5b) and thus any major redox processes in this region of Figure 5a can only be assigned as involving directly the isocorrole, (TT-10-isoCor)M or (TT-10-isoCor)H_2.

The singly and doubly oxidized isocorroles are relatively stable on the cyclic voltammetry timescale but this is not the case upon reduction where a chemical reaction follows electron addition, leading to an irreversible process and a product having electrochemical properties similar to that of the singly reduced corroles, $[(TTCor)Ni]^{-}$ and $[(TTCor)Cu]^{-}$. The first irreversible reduction of (TT-10-isoCor)Ni and (TT-10-isoCor)Cu both occur at the same potential of $E_{pc} = -0.92$ V and the peak current is slightly increased as compared to the two oxidations. On the return sweep there is no reoxidation associated with the reduction at −0.92 V but a reversible oxidation/reduction process is seen at exactly the same $E_{1/2}$ value as for reduction and reoxidation of the corresponding (TTCor)M derivatives, namely −0.03 V for M = Ni and −0.23 V for M = Cu, thus implying an isocorrole to corrole conversion upon reduction and reoxidation of these two compounds.

An electrochemically initiated isocorrole to corrole conversion is also suggested by cyclic voltammograms of the other examined isocorroles as illustrated in Figure 6 for (TT-5-isoCor)H_2 and (TT-5-isoCor)Ni and Figure 5a for (TT-10-isoCor)H_2. Unlike the Ni(II) and Cu(II) derivatives in Figure 5a, a well-defined second one electron reduction is observed for the other isocorroles with the difference in potential between the two one-electron additions ranging from 240 – 300 mV for the free-base derivatives and 410 mV for the Ni isocorrole. These separations are similar to the $\Delta E_{1/2}$ values observed between potentials for formation of porphyrin π anion radicals and dianions.[35] It should also be noted that the oxidation peak seen at $E_p = -0.06$ V after reduction of the two free-base isocorroles is not obtained if the scan is terminated prior to the first reduction and is located at a potential consistent with the $[(TTCor)H_2]^{-}/(TTCor)H_2$ redox reactions previously characterized for a variety of substituted corroles under the same solution conditions.[36] This suggests an isocorrole to corrole conversion also occurs in the case of the two free-base derivatives.

Finally, it should be pointed out that reductions of the 5-isocorroles are easier than the 10-isocorroles by 160 mV in the case of the two free-base derivatives and by ~ 230 mV in the case of the Ni complex but almost no differences are seen in the potentials for oxidation as shown by the data in Table 1 and Figure 7 which illustrates cyclic voltammograms of the two Ni isocorroles in PhCN. As seen in this figure, (TT-5-isoCor)Ni exhibits a reversible first oxidation at 0.70 V and an almost reversible first reduction, giving a HOMO-LUMO gap of 1.37 V. This compares to a gap of ~ 1.62 V for the (TT-10-isoCor)Ni in PhCN or 1.63 V for the same compound in CH_2Cl_2. The HOMO-LUMO gap of the isocorroles is in each case smaller than values for the related corroles which average 2.20 V under the same solution conditions.

In summary, the cyclic voltammograms of the five isocorroles are self-consistent in indicating an electrochemically initiated isocorrole to corrole conversion and this was confirmed by the thin-layer spectroelectrochemistry data. The proposed mechanism is given in Scheme 2 for the copper and free-base derivatives and may also be true for the nickel derivatives although some difference in the intermediate may exist as described on the following pages.

Spectroelectrochemistry

Thin-layer UV-visible spectroelectrochemistry was carried out in CH_2Cl_2, 0.1 M TBAP and an example of the spectral changes monitored during reduction of (TT-10-isoCor)Cu and (TTCor)Cu are illustrated in Figure 8. The spectrum of (TT-10-isoCor)Cu in CH_2Cl_2 is shown by the solid line in Figure 1. There are three bands at 372, 474 and 833 nm, all of which are assigned to the isocorrole and also another band at 417 nm which is due to trace (TTCor)Cu in solution. This spectrum is identical to the UV-vis spectrum obtained in CH_2Cl_2 containing 0.1 M TBAP as supporting electrolyte (Figure 8a). A potential of −0.50 V was then applied to the solution in the thin-layer cell and the isocorrole bands remain

unchanged, with the only difference in the spectrum being a loss of the formal Cu(III) corrole band at 417 nm and an increase in the Cu(II) corrole band at 432 nm (see Figure 8a). This contrasts with the much larger spectral changes which result upon switching to a controlled reducing potential of −1.10 V. As this reduction processes, all bands assigned to the isocorrole disappear and the final spectrum is characterized by an intense band at 432 and smaller bands at 573 and 609 nm. An identical spectrum is obtained upon the one-electron reduction of genuine (TTCor)Cu at −0.50 V (Figure 8b), thus indicating the same $[(TTCor)Cu]^-$ corrole product is formed upon electroreduction of both compounds.

Although the UV-vis spectra of the unreduced free-base 5-isocorrole and 10-isocorrole are quite different in CH_2Cl_2 (see Experimental section) exactly the same UV-vis spectrum is obtained after controlled potential reduction of the two compounds in the thin layer cell. Furthermore, the spectrum at the completion of electrolysis is the same as the spectrum of $[(TTCor)H_2]^-$ generated by reduction and proton loss from $(TTCor)H_3$ in PhCN (see Table 2).[36] This is consistent with the mechanism proposed in Scheme 2b and indicates that both isomers of the free-base isocorroles are converted to the same singly reduced diprotic corrole upon reduction. The electrogenerated $[(TTCor)H_2]^-$ product is relatively stable and can be reversibly oxidized to give $(TTCor^{\bullet})H_2$ (λ_{max} = 391 and 431 nm) and then rereduced to give $[(TTCor)H_2]^-$ again under the given experimental conditions.[36] The spectral changes which occur at each potential are shown in Fig. 9 and a summary of the spectral data before and after reduction and reoxidation are given in Table 2.

An isocorrole to corrole conversion is also seen for the two nickel derivatives whose cyclic voltammograms are shown in Figure 7. The UV-vis spectrum of the neutral isocorroles are quite different but identical spectra are obtained after controlled potential reduction in the thin-layer cell. This is shown in the top of Figure 10 where the product of reduction in each case is characterized by a Soret band at 416 nm, a Q band at 588 nm and a shoulder at 547 nm.

Although the electrogenerated product of the nickel isocorrole reductions is the same for each isomer, these spectra are not identical to the spectrum obtained in the first reduction of genuine (TTCor)Ni (Figure 10, bottom right), the main difference being in the Q band region. Nonetheless a controlled potential reoxidation of the electroreduced (TT-5-isoCor)Ni and (TT-10-isoCor)Ni shows quantitatively the formation of (TTCor)Ni in each case, thus again confirming an isocorrole to corrole conversion as also occurs with the copper and free-base derivatives. This mechanism for the two nickel isocorroles is shown in Scheme 3.

Conclusions

The reaction of 5- and 10-methoxy–isocorrole derivatives with different metal ions has been investigated with the aim to elucidate the coordination behavior of corrole analogs. The stability of the final isocorrole complex depends upon the central metal ion; if a formal oxidation state higher than the +2 is accessible to the coordinated metal ion, such as in the case of Co and Mn, a metal-to-ligand charge transfer occurs, which involves a reduction of the isocorrole species with the consequent rearomatization to the corresponding corrole complex. Stable isocorrole complexes have been obtained in the case of Cu and Ni ions.

Electrochemistry and spectroelectrochemistry characterization of free bases, Cu and Ni isocorrole derivatives provides further insight into the redox behavior of such a species, confirming the isocorrole to corrole conversion upon electroreduction.

Supplementary Material

Refer to Web version on PubMed Central for supplementary material.

Acknowledgments

We gratefully acknowledge the support of MIUR, Italy (PRIN project 2007C8RW53), the International Technology and Science Cooperation Foundation (BZ2007058, GJ2007006), the NSF (BK2008226) of Jiangsu Province, China, the US National Institutes of Health (K.M.S., Grant CA132861), and the Robert A. Welch Foundation (K.M.K., Grant E-680).

REFERENCES

1. Sessler, JL.; Gebauer, A.; Weghorn, SJ. The Porphyrin Handbook. Kadish, KM.; Smith, KM.; Guilard, R., editors. Vol. Vol. 2. San Diego: Academic Press; 2000. p. 55-124.
2. Latos-Grażyński, L. The Porphyrin Handbook. Kadish, KM.; Smith, KM.; Guilard, R., editors. Vol. Vol. 2. San Diego: Academic Press; 2000. p. 361-416.
3. Sessler, JL.; Weghorn, SJ. Expanded, Contracted and Isomeric Porphyrins. Pergamon, Oxford: 1997.
4. Sessler, JL.; Gebauer, A.; Vogel, E. The Porphyrin Handbook. Kadish, KM.; Smith, KM.; Guilard, R., editors. Vol. Vol. 2. San Diego: Academic Press; 2000. p. 1-54.
5. Woodward RB. Ind. Chim. Belge 1962;27:1293–1308.
6. Gross Z, Gray HB. Adv. Synth. Catal 2004;346:165–170.
7. Aviv I, Gross Z. Chem. Commun 2007:1987–1999.
8. Barbe J-M, Canard G, Brandès S, Jérome F, Dubois G, Guilard R. J. Chem. Soc., Dalton Trans 2004:1208–1214.
9. Paolesse, R.; Mandoj, F.; Marini, A.; Di Natale, C. Encyclopedia of Nanoscience and Nanotechnology. Nalwa, H., editor. Vol. Vol. 9. Valencia, CA: American Science Publishers; 2004. p. 21-42.
10. Setsune JI, Tsukajima A, Watanabe J. Tetrahedron Lett 2006;47:1817–1820.
11. Hohlneicher G, Bremm D, Wytko J, Bley-Escrich J, Gisselbrecht J-P, Gross M, Mechels M, Lex J, Vogel E. Chem. Eur. J 2003;9:5636–5642.
12. Setsune JI, Tsukajima A, Okazaki N. J. Porphyrins Phthalocyanines 2009;13:256–265.
13. Will S, Rahbar A, Schmickler H, Lex J, Vogel E. Angew. Chem., Int. Ed. Engl 1990;29:1390–1393.
14. Vogel E, Binsack B, Hellwig Y, Erben C, Heger A, Lex J, Wu Y-D. Angew. Chem., Int. Ed 1997;36:2612–2615.
15. Orlewska C, Maes W, Toppet S, Dehaen W. Tetrahedron Lett 2005;46:6067–6070.
16. Nardis S, Pomarico G, Fronczek FR, Vicente MGH, Paolesse R. Tetrahedron Lett 2007;48:8643–8646.
17. Gross Z, Galili N, Saltsman I. Angew. Chem., Int. Ed 1999;38:1427–1429.
18. Paolesse R, Jaquinod L, Nurco DJ, Mini S, Sagone F, Boschi T, Smith KM. Chem. Commun 1999:1307–1308.
19. Paolesse R, Nardis S, Sagone F, Khoury R. J. Org. Chem 2001;66:550–556. [PubMed: 11429828]
20. Koszarna B, Gryko DT. J. Org. Chem 2006;71:3707–3717. [PubMed: 16674040]
21. Flint DL, Fowler RL, LeSaulnier TD, Long AC, O'Brien AY, Geier GR III. J. Org. Chem. 2010 ASAP.
22. Spek AL. J. Appl. Cryst 2003;36:7–13.
23. (a) Paolesse, R. The Porphyrin Handbook. Kadish, KM.; Smith, KM.; Guilard, R., editors. Vol. Vol. 2. San Diego: Academic Press; 2000. p. 201-232.(b) Erben, C.; Will, S.; Kadish, KM. The Porphyrin Handbook. Kadish, KM.; Smith, K.; Guilard, R., editors. Vol. Vol. 2. San Diego: Academic Press; 2000. p. 233-300.
24. Paolesse R, Jaquinod L, Senge MO, Smith KM. J. Org. Chem 1997;62:6193–6198.
25. Luobeznova I, Simkhovich L, Goldberg I, Gross Z. Eur. J. Inorg. Chem 2004;8:1724–1732.
26. Vogel E, Will S, Tilling AS, Neumann L, Lex J, Bill E, Trautwein AX, Wieghardt K. Angew. Chem., Int. Ed. Engl 1994;33:731–735.

27. Wasbotten IH, Wondimagegn T, Ghosh A. J Am. Chem. Soc 2002;124:8104–8116. [PubMed: 12095356]
28. Brückner C, Briñas RP, Krause Bauer JA. Inorg. Chem 2003;42:4495–4497. [PubMed: 12870931]
29. Guilard R, Gros CP, Barbe JM, Espinosa E, Jérôme F, Tabard A. Inorg. Chem 2004;43:7441–7455. [PubMed: 15530095]
30. Bröring M, Brégier F, Consul Tejero E, Hell C, Holthausen MC. Angew. Chem., Int. Ed 2007;46:445–448.
31. Allen FH. Acta Cryst 2002;B58:380–388.
32. He H-S. Acta Cryst 2007;E63:m976–m977.
33. Senge MO, Bischoff I, Nelson NY, Smith KM. J. Porphyrins Phthalocyanines 1999;3:99–116.
34. Ou Z, Shao J, Zhao H, Ghosh A, Kadish KM. J. Porphyrins Phthalocyanines 2004;8:1236–1247.
35. Kadish, KM. The Porphyrin Handbook. Kadish, KM.; Smith, KM.; Guilard, R., editors. Vol. Vol. 8. San Diego: Academic Press; 2000. p. 1-97.
36. Shen J, Shao J, Ou Z, E W, Koszarna B, Gryko DT, Kadish KM. Inorg. Chem 2006;45:2251–2265. [PubMed: 16499391]

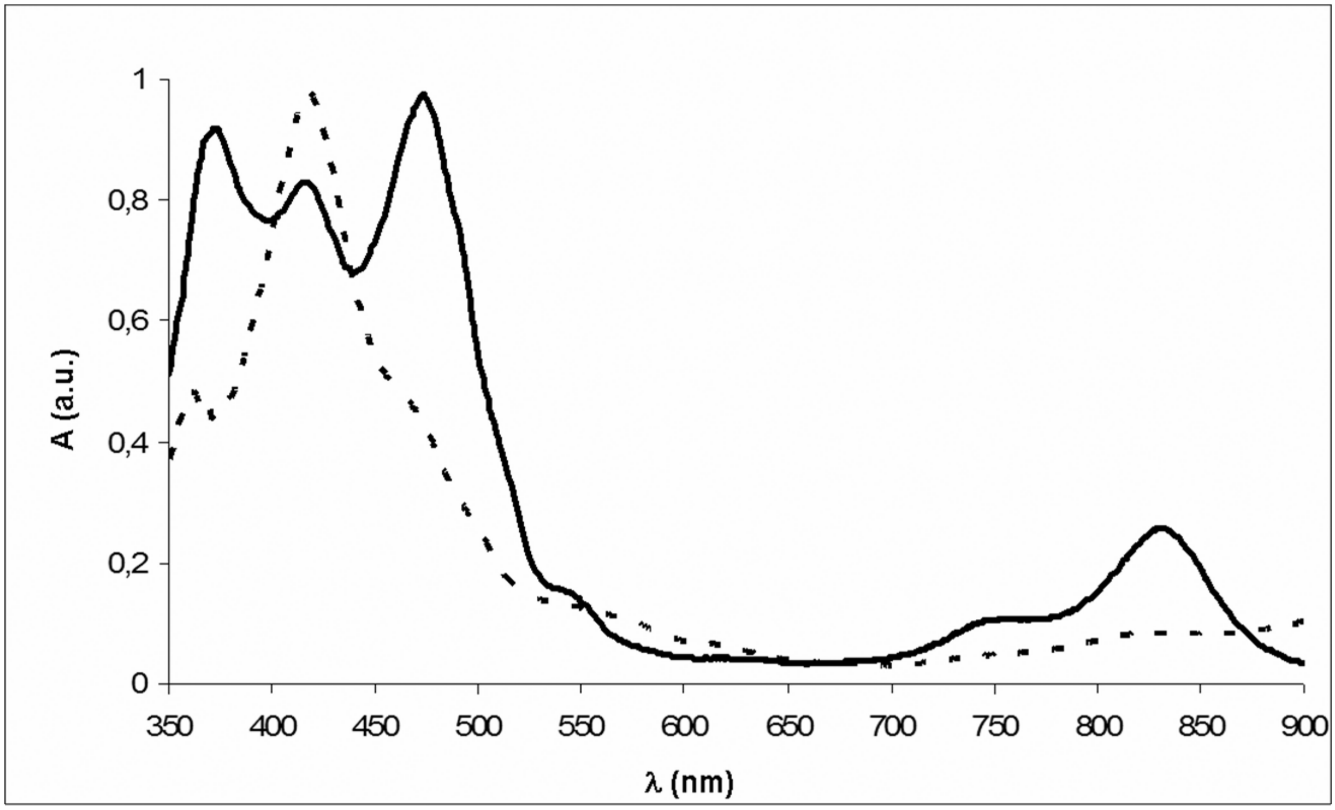

Figure 1.
UV-vis spectra of (TT-10-isoCor)Cu (solid line) and of (TT-5-isoCor)Cu (dotted line).

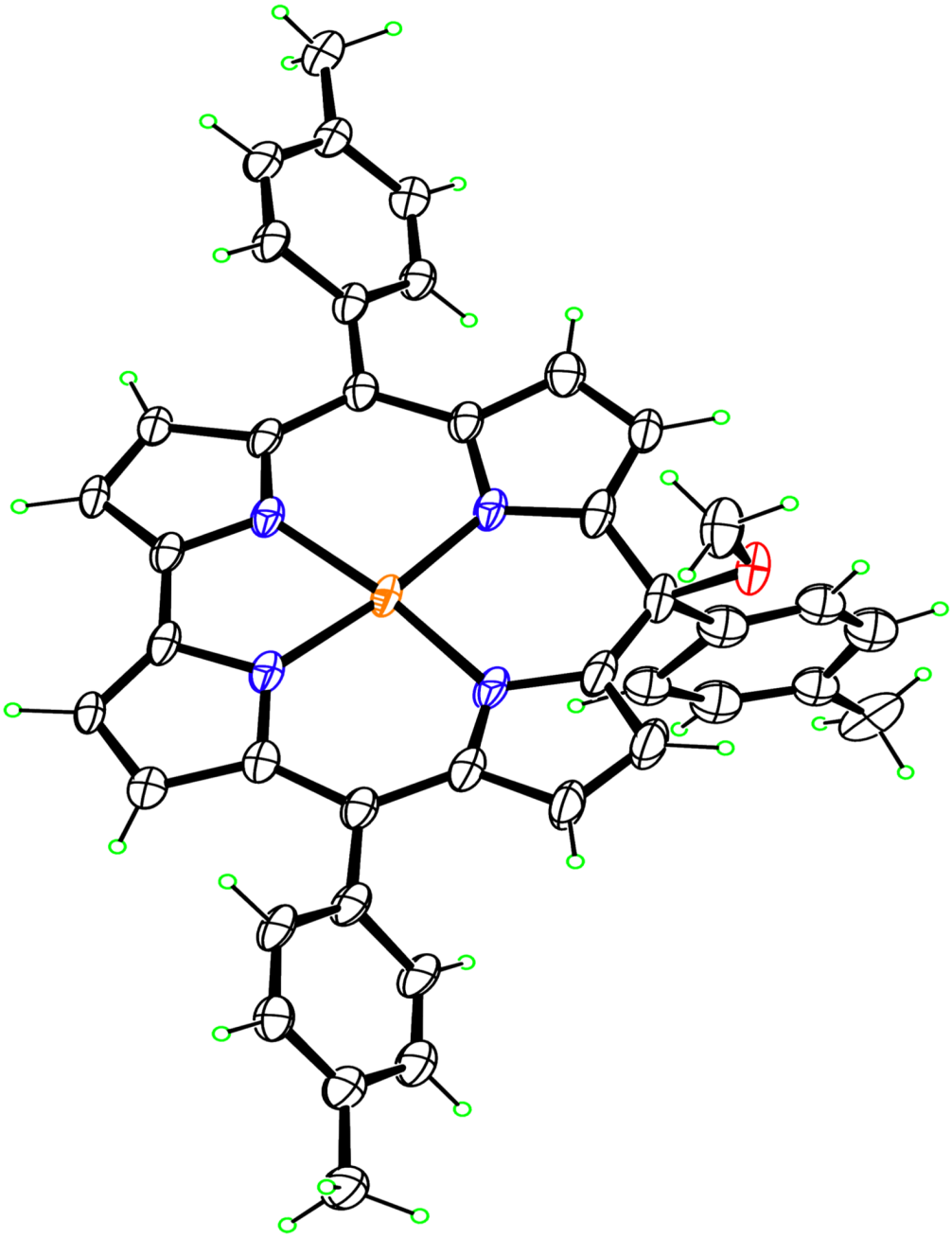

Figure 2.
X-ray molecular structure of (TT-10-isoCor)Cu.

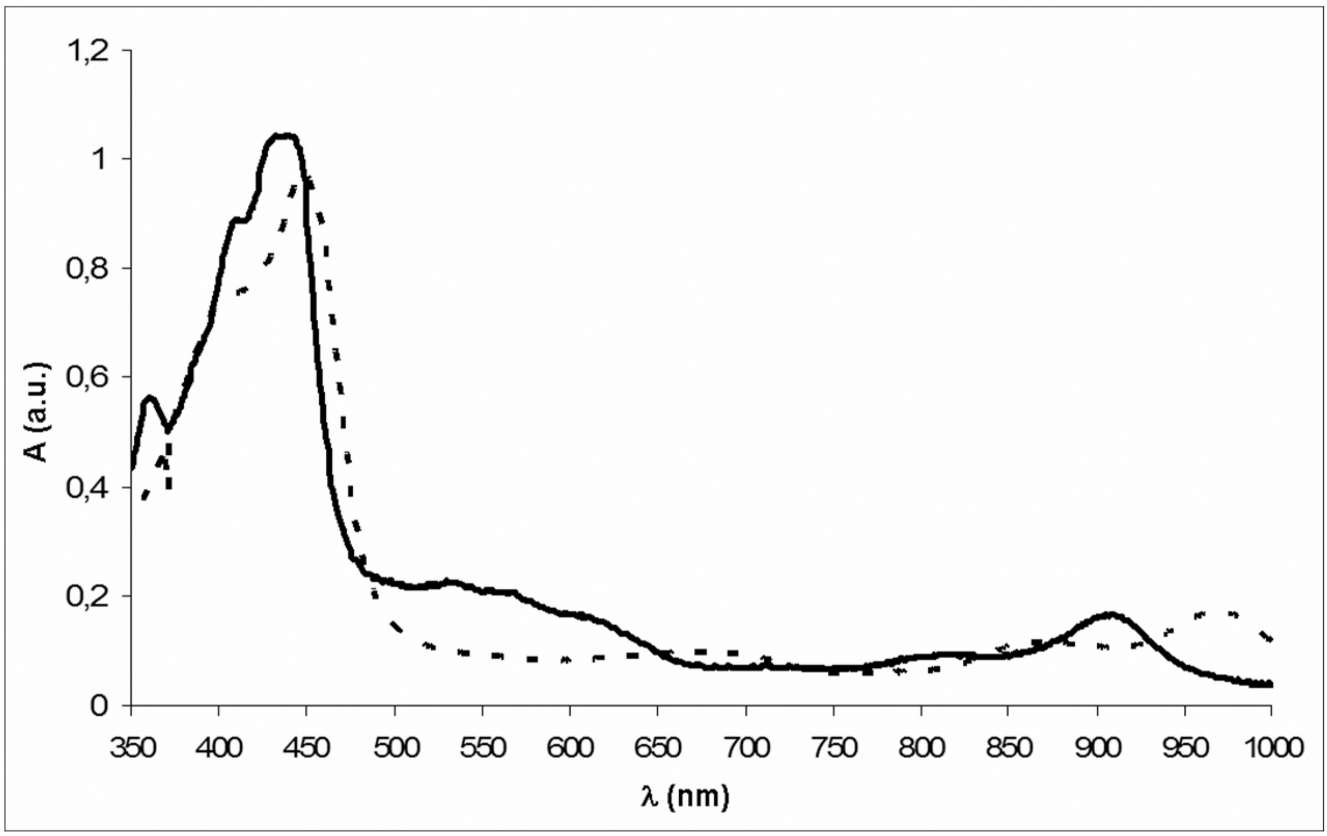

Figure 3.
UV-vis spectra of (TT-10-isoCor)Ni (−−) and of (TT-5-isoCor)Ni (----).

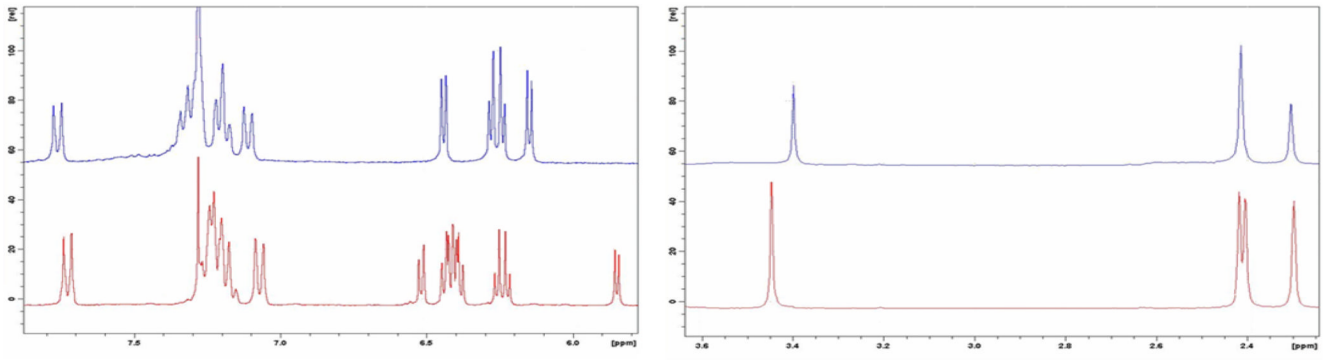

Figure 4.
^{1}H NMR spectra of (TT-10-isoCor)Ni (up) and of (TT-5-isoCor)Ni (down).

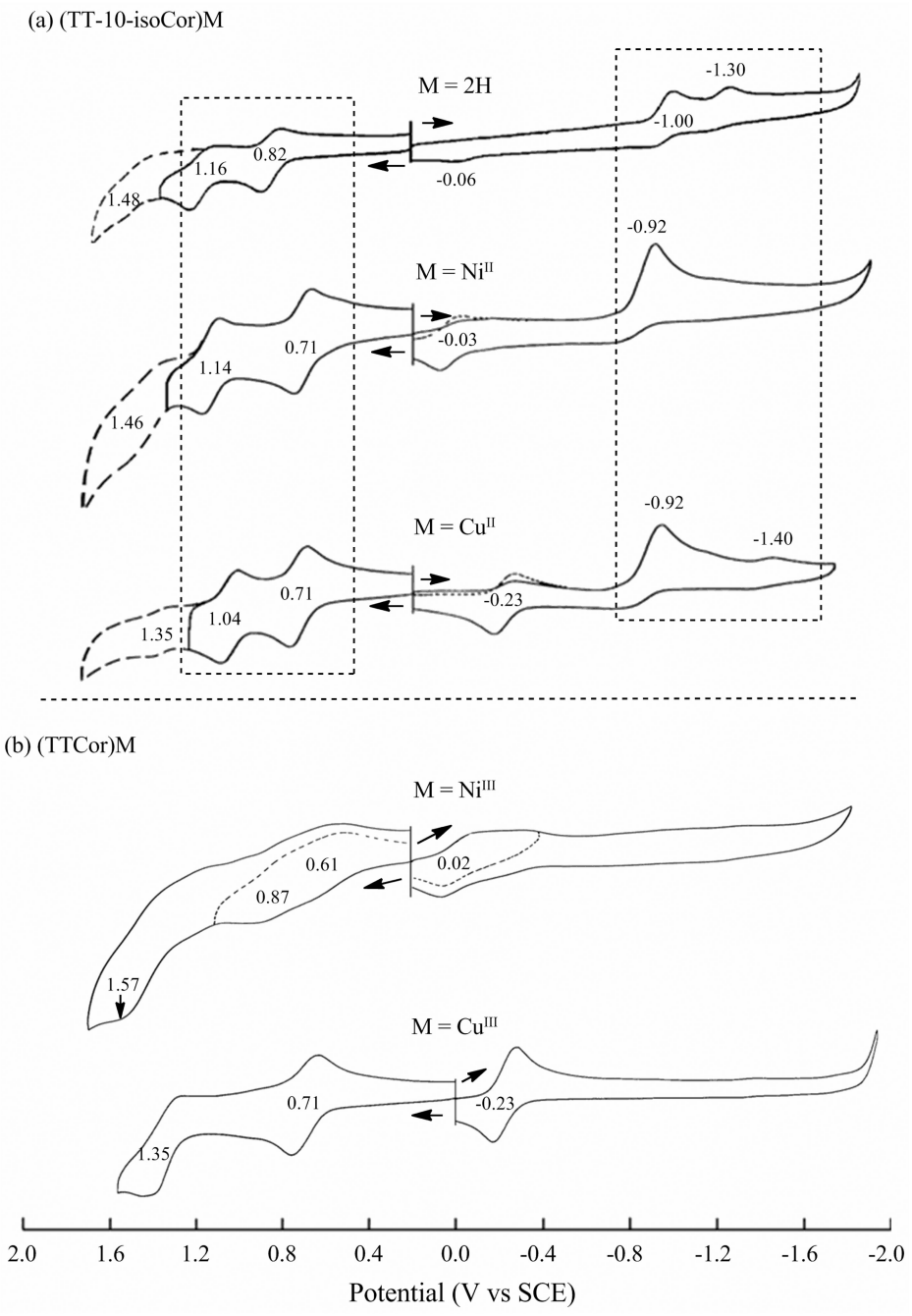

Figure 5.

Cyclic voltammograms of (a) (TT-10-isoCor)M and (b) (TTCor)M in CH_2Cl_2, 0.1 M TBAP. Reactions within the “boxes” of Figure 5a are those assigned to the isocorroles, all others being assigned to oxidation or reduction of a (TTCor)M “side product”.

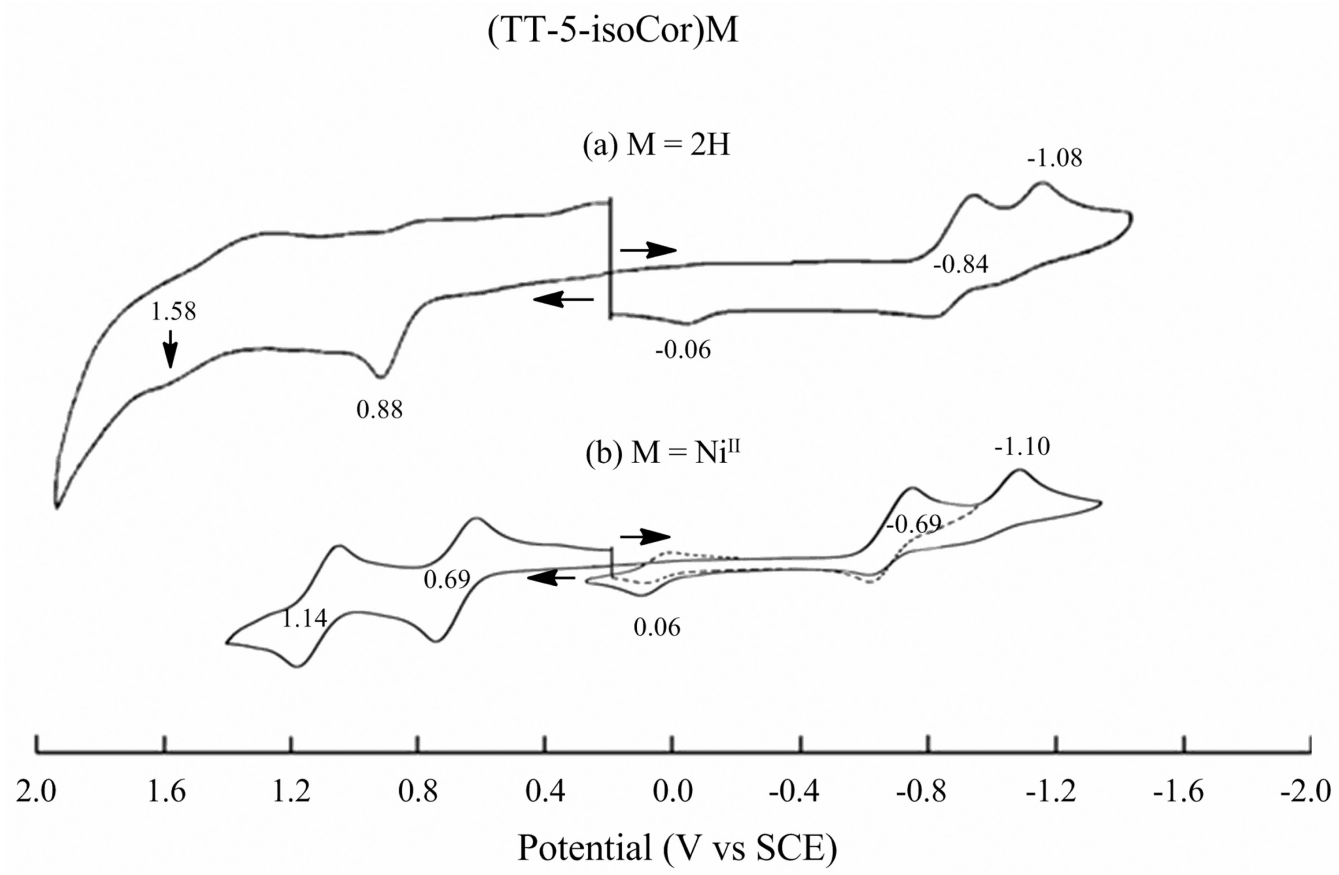

Figure 6.
Cyclic voltammograms of (TT-5-isoCor)M, (a) M = 2H and (b) M = Ni^{II} in CH_2Cl_2, 0.1 M TBAP.

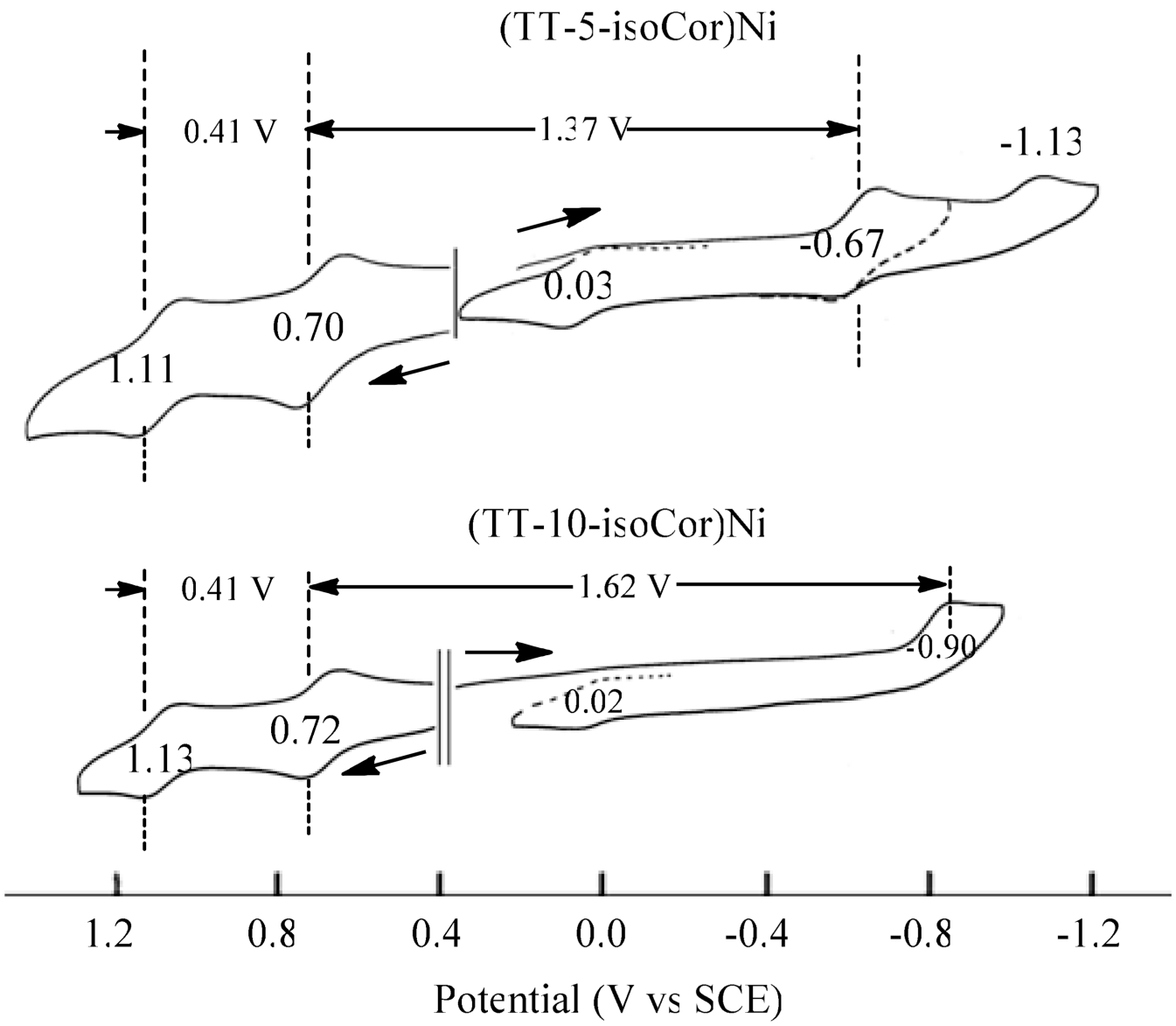

Figure 7.
Cyclic voltammograms of (TT-5-isoCor)Ni and (TT-10-isoCor)Ni in PhCN, 0.1 M TBAP.

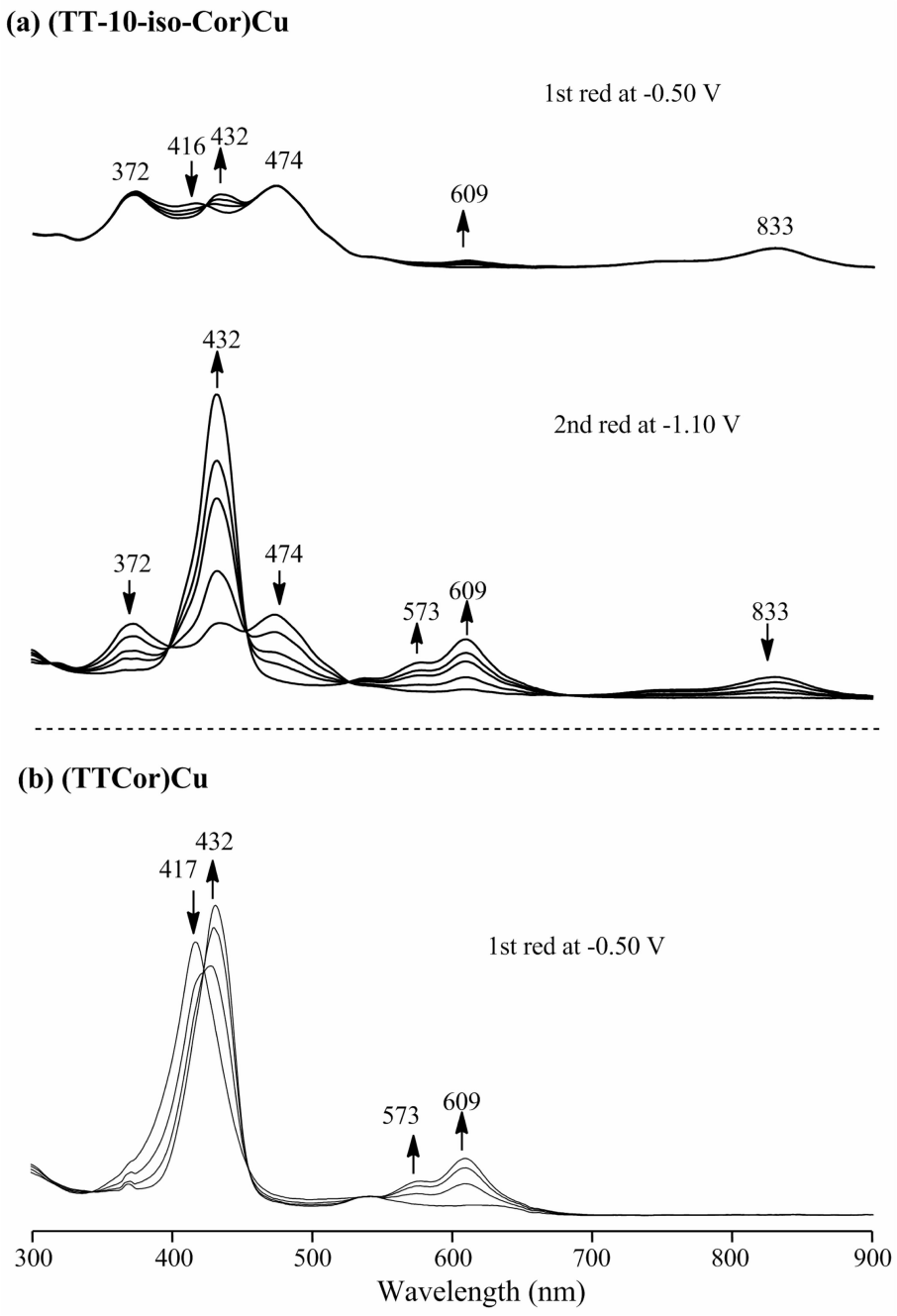

Figure 8.

UV-vis spectral changes obtained during the reductions of (a) (TT-10-isoCor)Cu and (b) (TTCor)Cu in CH_2Cl_2, 0.1 M TBAP. The bands at 432, 573 and 609 nm are attributed to the anionic corrole while the 417 nm band is associated with the unreduced Cu(III) corrole.

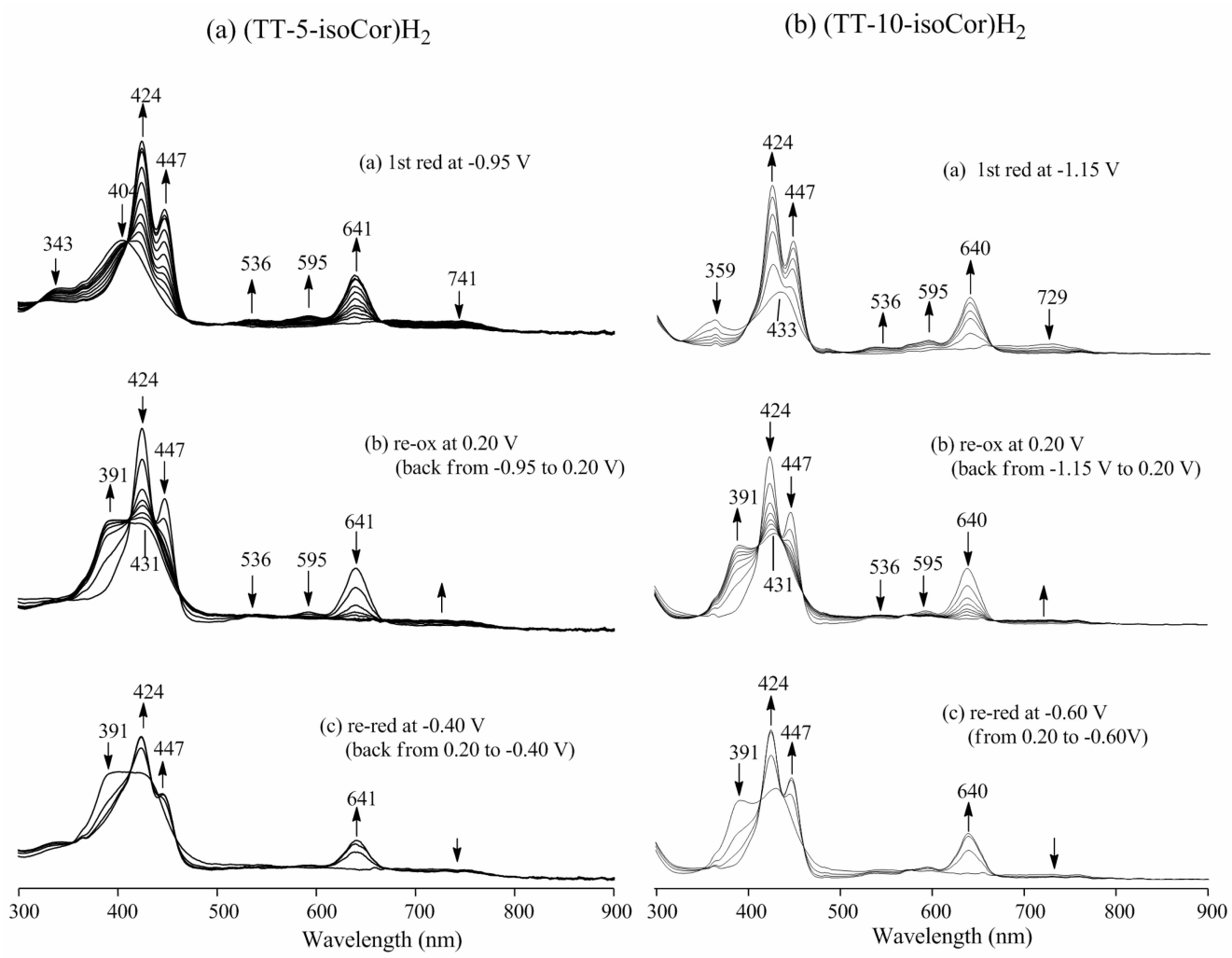

Figure 9.

UV-vis spectral changes obtained upon stepwise controlled potential reduction, re-oxidation and re-reduction for (a) (TT-5-isoCor)H_2 and (b) (TT-10-isoCor)H_2 in CH_2Cl_2, 0.1 M TBAP.

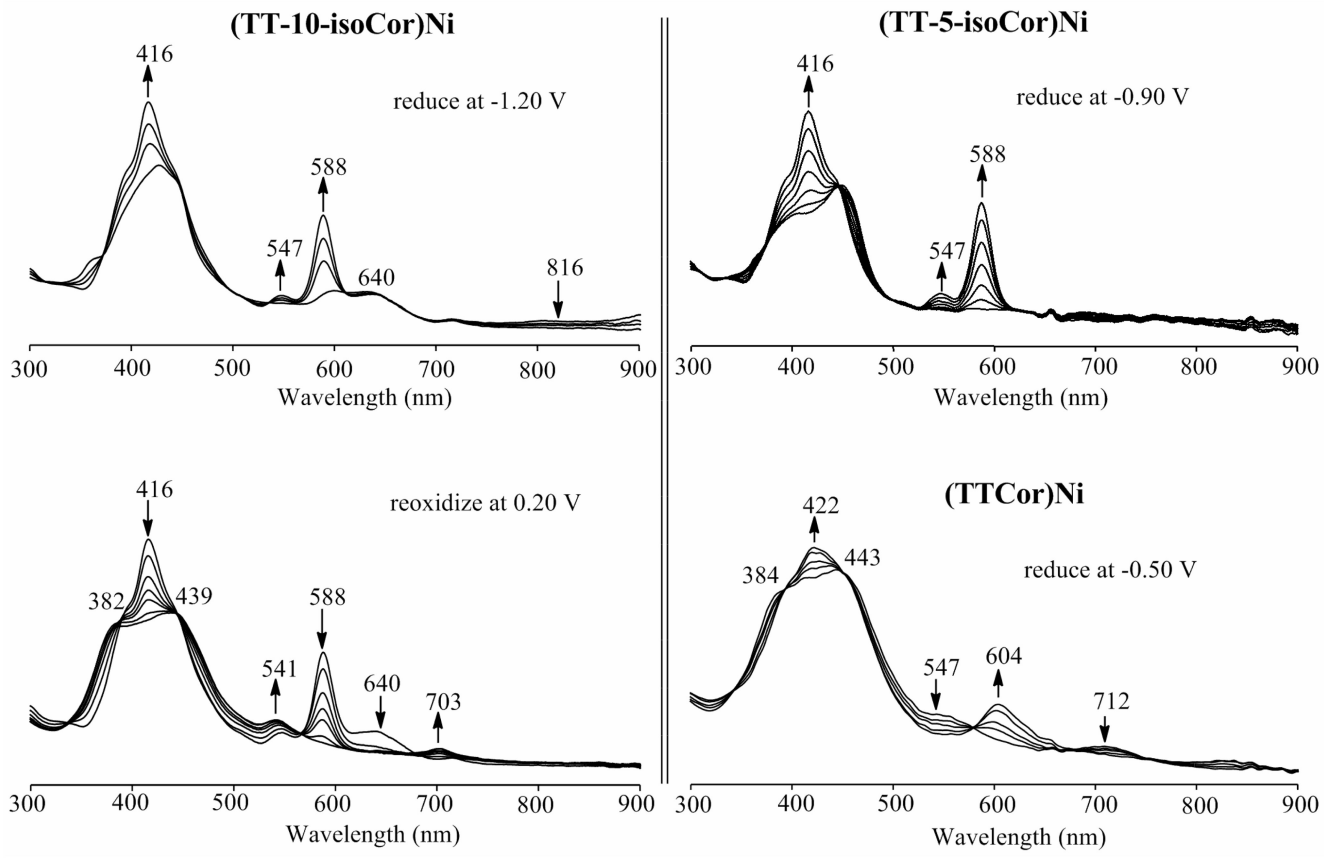

Figure 10.

Spectral changes during controlled potential reduction of (TT-10-isoCor)Ni and (TT-5-isoCor)Ni in a thin-layer cell (top) with comparison to the reoxidation product at E_{app} = 0.20 V (bottom left) and genuine (TTCor)Ni in its neutral and singly reduced forms (bottom right).

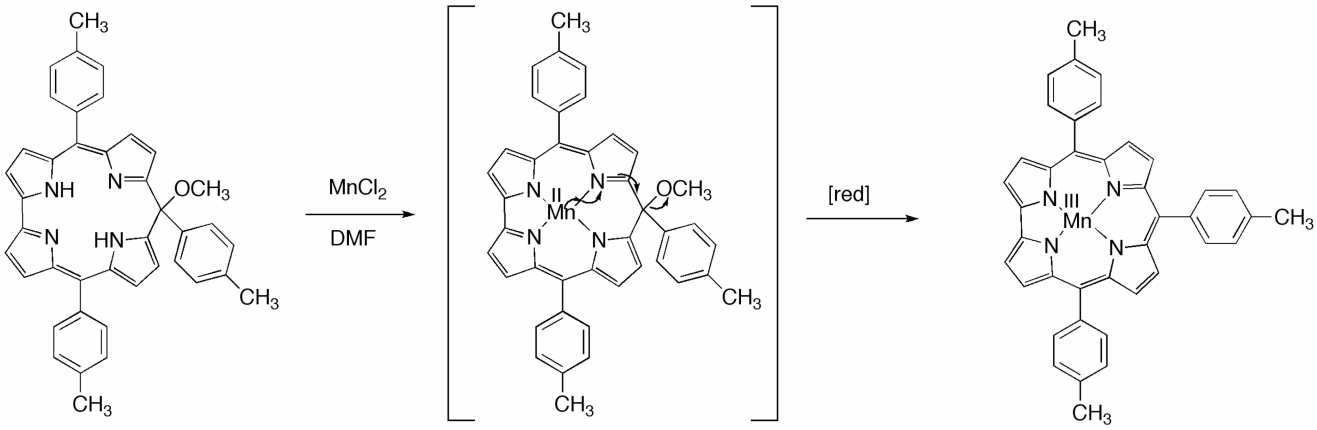

Scheme 1.
The pathway of conversion an isocorrole to a corrole.

(a)

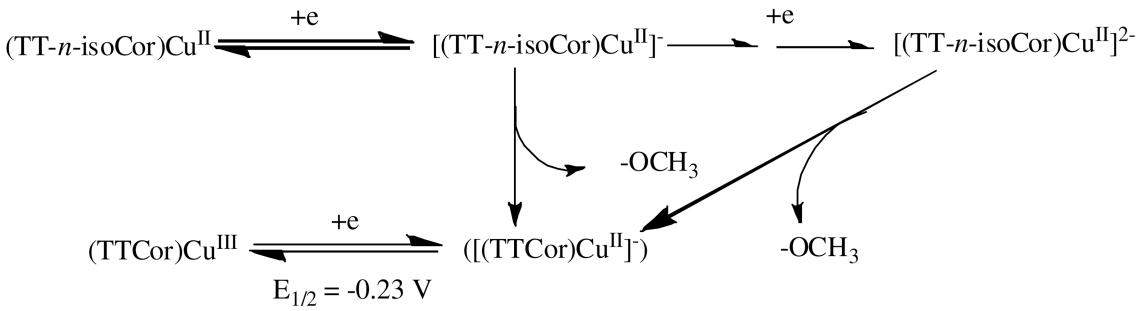

(b)

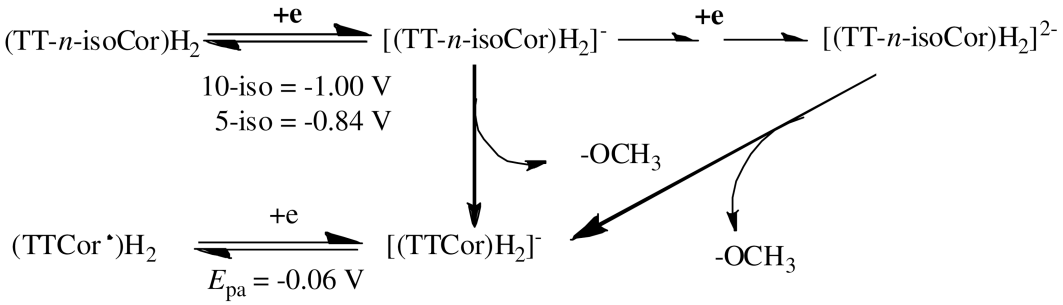

Scheme 2.

Proposed reduction mechanism of (a) copper isocorroles and (b) free-base 5- and 10-isocorroles in CH_2Cl_2, 0.1 M TBAP.

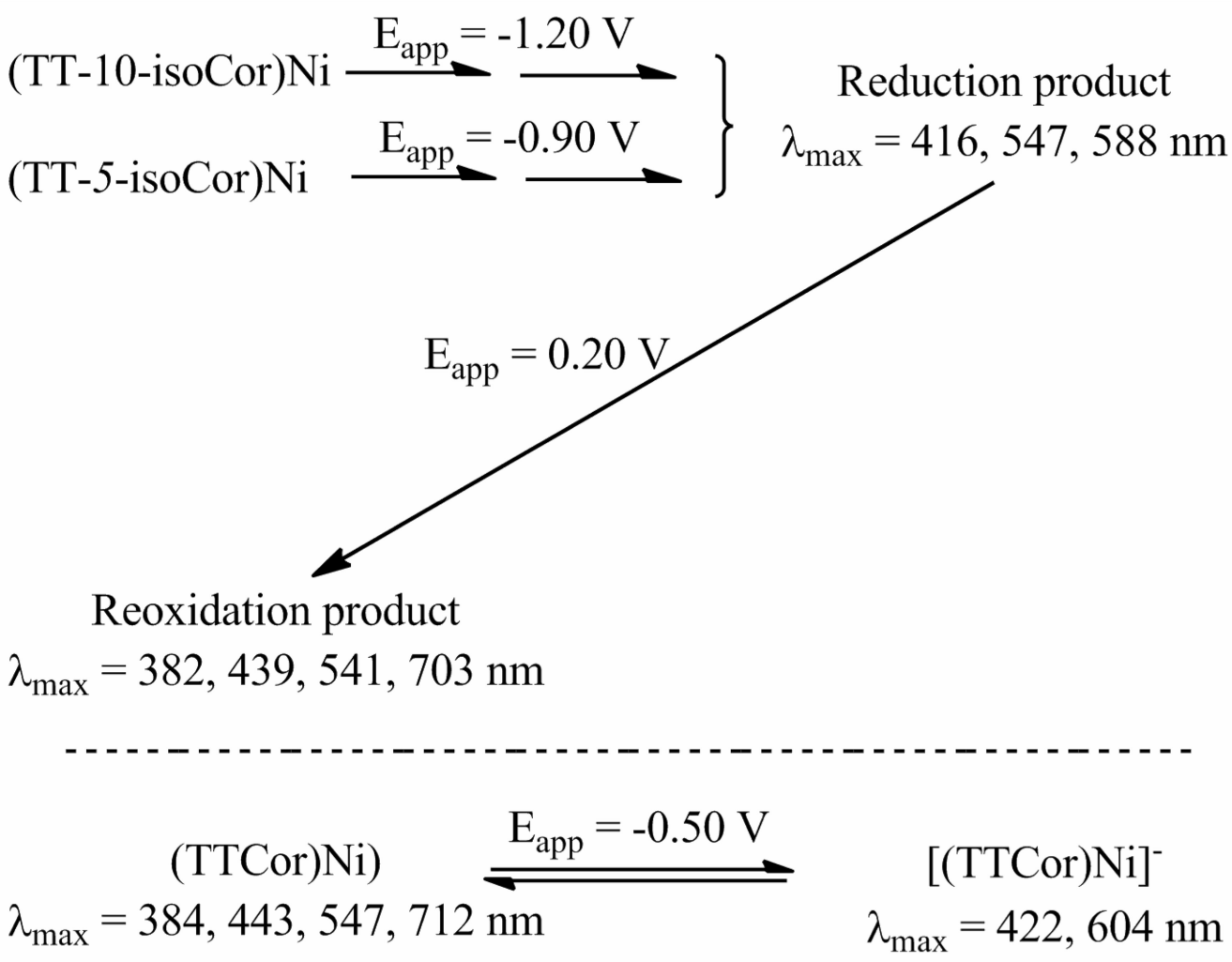

Scheme 3.

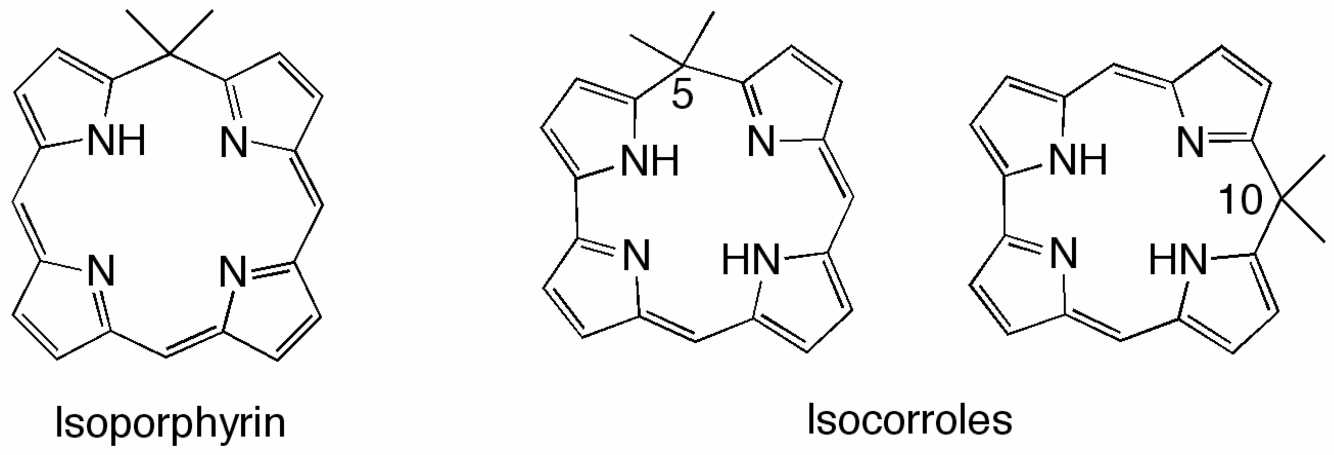

Chart 1.
Structure of isoporphyrin (left) and isocorroles (center and right)

Table 1

Half-wave Potentials (V vs SCE) of Isocorroles and Related Corroles in CH_2Cl_2, 0.1 M TBAP.

Macrocycles	Central metal	Oxidation			Reduction		
		$\Delta E_{2\text{-}1}$	2nd	1st	1st	2nd	$\Delta E_{1\text{-}2}$
TT-10-isoCor	2H	0.34	1.16	0.82	−1.00	−1.30[a]	0.30
	Ni^{II}	0.43	1.14	0.71	−0.92[a]	−1.26[a]	0.34
	Cu^{II}	0.33	1.04	0.71	−0.92[a]	−1.40[a]	0.48
TT-5-isoCor	2H	0.70	1.58[a]	0.88[a]	−0.84	−1.08[a]	0.24
	Ni^{II}	0.45	1.14	0.69	−0.69	−1.10[a]	0.41
TTCor	Ni^{III}	---	1.57[a]	0.87[c], 0.61	0.02	---	---
	Cu^{III},[b]	0.65	1.35	0.70	−0.23	---	---

[a] Irreversible peak potential at a scan rate of 0.10 V/s.

[b] Data taken from ref 34.

[c] Split peaks due to dimerization.

Table 2

UV-visible Data (λ_{max}, nm) of Electrogenerated $[(TTCor)H_2]^-$ and $(TTCor^{\bullet})H_2$.

Starting compound	Solvent	1st red product $[(TTCor)H_2]^-$					Ox prod. $(TTCor^{\bullet})H_2$	
		Soret region		visible region			Soret region	
(TT-10-isoCor)H_2	CH_2Cl_2	424	447	536	595	640	391	431
(TT-5-isoCor)H_2	CH_2Cl_2	424	447	536	595	641	391	431
(TTCor)H_3[a]	PhCN	430	452	536	596	644	396	436

[a]Data taken from ref 36.